Photophysical Properties of C_{60} Colloids Suspended in Water with Triton X-100 Surfactant: Excited-State Properties with Femtosecond Resolution

Andrew F. Clements,*,† Joy E. Haley,*,‡,§ Augustine M. Urbas,‡ Alan Kost,|| R. David Rauh,⊥ Jane F. Bertone,⊥ Fei Wang,⊥ Brian M. Wiers,# De Gao,# Todd S. Stefanik,# Andrew G. Mott,▽ and David M. Mackie▽

US Army RDECOM-TARDEC, MS-263, 6501 E. 11 Mile Rd., Warren, MI 48397-5000, Materials and Manufacturing Directorate, Air Force Research Laboratory, WPAFB, OH 45433, UES, Inc., 4401 Dayton-Xenia Road, Dayton, Ohio 45432, University of Arizona, College of Optical Sciences, 1630 E. University Blvd., Tucson, AZ 85721-0094, EIC Laboratories, Inc., 111 Downey Street, Norwood, MA 02062, Nanocerox, Inc., 712 State Circle, Ann Arbor, MI 48108, and US Army Research Laboratory, Attn: AMSRD-ARL-SE-EM, 2800 Powder Mill Road, Adelphi, MD 20783-1197

Received: November 21, 2008; Revised Manuscript Received: April 6, 2009

We examine the photophysics of a colloidal suspension of C_{60} particles in a micellar solution of Triton X-100 and water, prepared via a new synthesis which allows high-concentration suspensions. The particle sizes are characterized by transmission electron microscopy and dynamic light scattering and found to be somewhat polydisperse in the range of 10−100 nm. The suspension is characterized optically by UV−vis spectroscopy, femtosecond transient absorption spectroscopy, laser flash photolysis, and z-scan. The ground-state absorbance spectrum shows a broad absorbance feature centered near 450 nm which is indicative of colloidal C_{60}. The transient absorption dynamics, presented for the first time with femtosecond resolution, are very similar to that of thin films of C_{60} and indicate a strong quenching of the singlet excited state on short time scales and evidence of little intersystem crossing to a triplet excited state. Laser flash photolysis reveals that a triplet excited-state absorption spectrum, which is essentially identical in shape to that of molecular C_{60} solutions, does indeed arise, but with much lower magnitude and somewhat shorter lifetime. Z-scan analysis confirms that the optical response of this material is dominated by nonlinear scattering.

Introduction

Since its discovery,[1] the uniquely symmetrical C_{60} molecule has been widely studied, and many applications for it and its derivatives have been proposed, notably lubricants,[2] superconductors,[3] sensors,[4−7] solar cells,[8] and biomedical applications[9−11] such as drug delivery and photodynamic therapy. In particular, the photophysical properties of the C_{60} molecule have been the subject of intense study. Many authors have reported on the photophysical properties of molecular solutions of C_{60}.[12−20] Likewise, many authors have studied the photophysical and structural properties of solid films of C_{60}.[21−34] Under certain conditions, C_{60} forms stable colloidal assemblies in solvents.[35−44] Colloidal suspensions of C_{60} particles can also be formed in binary solvent mixtures, in which one is a good solvent and the other is a poor solvent for C_{60}.[45−49] Aqueous suspensions of colloidal C_{60} particles are also formed by a number of methods,[50−64] including solubilization in micellar solutions.[55,61,65−69] Some studies have been done of the photophysical properties of these colloidal fullerene suspensions.[67,68,70,71] The photochemical properties, and in particular the generation of reactive oxygen species (ROS) via intersystem crossing to the triplet state, have been of interest both for potential exploitation for photodynamic therapy[9] and regarding concerns about their potential environmental impact, because there have been reports of significant cytotoxicity effects.[50−53]

This work reports on the excited-state dynamics of an aqueous suspension of C_{60} suspended in Triton X-100, as shown in Figure 1, to form stable aqueous colloids. These colloidal suspensions were synthesized via a new preparation method (modified from that reported in the literature by Deguchi)[44,63] which yields suspensions of high concentrations, on the order of 4 mM. We present, for the first time with femtosecond resolution, the transient absorption spectra and kinetic lifetimes of both the singlet and triplet excited states of concentrated aqueous C_{60} colloidal suspensions as well as the first z-scan results of such materials, compared to a molecular solution of C_{60} and a carbon black suspension.

Experimental Methods

Synthesis and Stock Concentration Determination. An aqueous suspension of C_{60} colloidal particles, solubilized by Triton X-100 micelles, was synthesized and evaluated in this study. An aqueous suspension of acidified carbon black nanoparticles and a molecular solution of C_{60} in toluene were used as reference materials for comparison.

C_{60}[Tol] 15:85 Triton X-100:H_2O. C_{60} (98% purity) was purchased, and a solution was prepared by dissolving 10 mg of C_{60} into 4 mL of toluene by stirring for 3 days. The UV−vis spectrum of this toluene solution was measured by using a 2 mm cell. The solution was diluted by 1:1 with neat toluene,

* Corresponding authors. E-mail: Andy.Clements@us.army.mil, Phone: 586-574-5389, FAX: 586-574-6145 and E-mail: Joy.Haley@wpafb.af.mil, Phone: 937-255-9718, FAX: 937-255-1128.
† US Army RDECOM-TARDEC.
‡ Air Force Research Laboratory.
§ UES, Inc.
|| College of Optical Sciences.
⊥ EIC Laboratories, Inc.
Nanocerox, Inc.
▽ US Army Research Laboratory.

10.1021/jp8102518 CCC: $40.75
Published on Web 05/14/2009

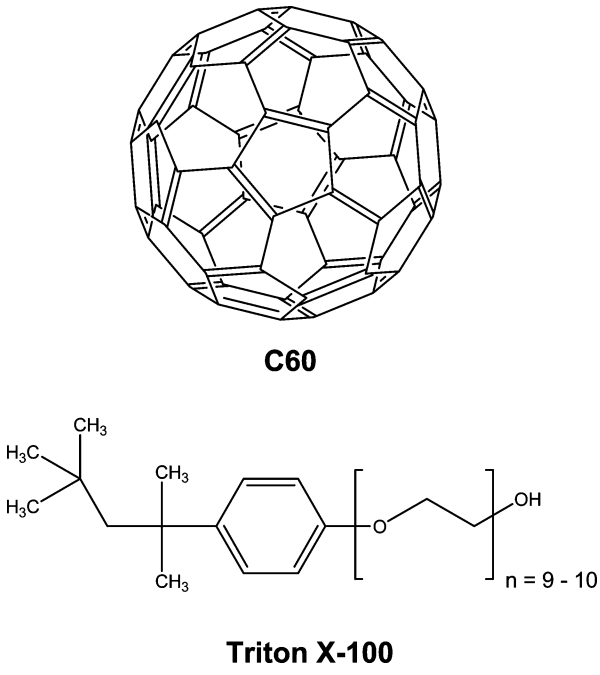

Figure 1. Structure of C_{60} and Triton X-100 surfactant.

and the UV−vis spectrum of the diluted sample was recorded. The dilutions were repeated two more times.

The absorbance at 532 nm was plotted against C_{60} concentration (mg/mL). The calibration curve obtained from the absorbance curve is

$$A_{532} = 0.2311 \times (C_{60}\text{in mg/mL}) + 0.0058 \qquad (1)$$

The absorbance at 532 nm was also plotted against C_{60} concentration in moles, and the molar extinction coefficient, ε, was obtained as 832 M^{-1} cm^{-1}. This value is consistent with data from the literature.[72]

The combined 7 mL of C_{60} toluene solution (including the diluted portions) was placed in a 16 mL wide mouth vial, and 0.3 mL of Triton X-100 was added. (Figure 1 depicts both the C_{60} and Triton X-100 molecules.) The vial was placed on a 50 °C water bath, and argon was bubbled through the solution. After 4 h, all toluene had evaporated, leaving a dark brown colored Triton X-100 and C_{60} residue in the vial. A total of 1.7 mL of deionized water (resistivity of 10−15 MΩ cm and TOC < 30 μg/L [ppb]) was then added to the residue in 0.7 and 1 mL increments, with sonication between additions. A dark brown suspension was formed, the color typical of C_{60} colloids, along with some precipitated C_{60} in the bottom of the vial. The suspension was filtered through a 0.22 μm syringe filter. About 1.9 mL of filtered solution was obtained.

The vial containing C_{60} residue, syringe filter, and syringe were dried under vacuum for 4 h. The syringe was washed by toluene to recover C_{60}. The filters were cut open, and the filter membrane was cut to small pieces and placed in the vial containing C_{60} residue. The mixture was extracted by toluene with stirring for 24 h. The total extracted volume of toluene was 4.2 mL. It was filtered by 0.2 μm syringe filter, and the UV−vis was collected. The absorbance at 532 nm was 0.325. The absorbance baseline, from 700 to 800 nm, is zero, indicating no scattering from particles. According to the calibration curve eq 1, this corresponds to C = 1.38 mg/mL. Thus, the total amount of C_{60} that was not extracted by Triton is 5.80 mg, leaving 4.20 mg of C_{60} extracted by the Triton in water. The initial C_{60} concentration in Triton/water was therefore 2.21 mg/mL.

Serial aqueous dilutions were made of this stock solution by using Triton/water (15% v/v) to yield solutions of 1.105, 0.553, 0.276, 0.138 mg/mL. Their UV−vis spectra were taken by using a 2 mm cell. The diluted samples appeared stable; no precipitation was observed overnight.

The absorbance at 532 nm was plotted against C_{60} concentration in molarity (mol/L). The Beer's Law plot yielded a molar extinction coefficient, ε, of 1289 M^{-1} cm^{-1}. When plotted against C_{60} in mg/mL, the following calibration curve was obtained:

$$A_{532} = 0.3579 \times (C_{60}\text{in mg/mL}) + 0.0126 \qquad (2)$$

The sample used in the experiments in this manuscript was determined to have an absorbance of 1.15 at 532 nm in a 2 mm path length. Therefore, the calculated C_{60} concentration in this sample, according to eq 2, is 3.18 mg/mL or 0.00441 M.

Acidified Carbon Black in Water. A suspension of carbon black in deionized water was prepared by using acid digestion to deagglomerate and functionalize carbon black particles with carboxylic acid groups. A total of 20 mL of concentrated ACS grade nitric acid (70%) and 30 mL of concentrated ACS grade sulfuric acid (95−98%) were placed in a 500 mL beaker. To this mixture, 1 g of carbon black (Cabot Monarch-1000, ~300 m^2/g) was added. Addition was carried out slowly with swirling of the solution to avoid ignition of the carbon. This mixture was warmed to low temperature on a hot plate, resulting in the evolution of orange vapors. After approximately 1 h, vapor evolution subsided, and a brown, oil-like substance remained. This material was rinsed into a round-bottom flask by using deionized water and heated to distill off excess acid. The residue remaining was transferred to a beaker. The material was rinsed twice by adding deionized water, sonicated to disperse, then heated to evaporate to dryness. Water was added a third time, followed by sonication, then centrifugation to remove large particles. The supernatant was collected, and the remaining water was evaporated. A total of 0.033 g of the resulting solid was dispersed in 5 mL deionized water to form the carbon black suspension used in these studies.

Particle Characterization by TEM. Particle size characterization was conducted by using a 200 kV transmission electron microscope (TEM). Statistics were obtained by manually measuring the sizes of all particles in the images, by using statistical software.

Particle-Size Distribution by DLS. Particle-size distribution was also measured by dynamic light scattering (DLS). For undiluted samples, the viscosity input to the DLS instrument was determined for the ratio of Triton-X-100 to water in the sample by interpolation of viscosity data available on the DOW Answer Center knowledge base.[73] For diluted samples, the viscosity was very near that of water. The refractive index was set at 2.2 for the C_{60} DLS measurements, in accordance with the literature.[55,74] The refractive index was set at 1.85 for the carbon black sample.[75,76]

Ground-State Absorbance. Ground state UV−vis absorption spectra were measured on a spectrophotometer in a 1 mm path length quartz cuvette.

Ultrafast Transient Absorption. Ultrafast pump−probe transient absorption measurements were performed by using a commercially available femtosecond pump−probe UV−vis spectrometer. Briefly, 1 mJ, 170 fs pulses at 780 nm at a 500 Hz repetition rate were obtained from a Ti:sapphire laser. The output laser beam was split into pump and probe by a beam splitter. The pump beam was directed into a frequency doubler (390 nm) and then focused into the sample. The probe beam was delayed in a

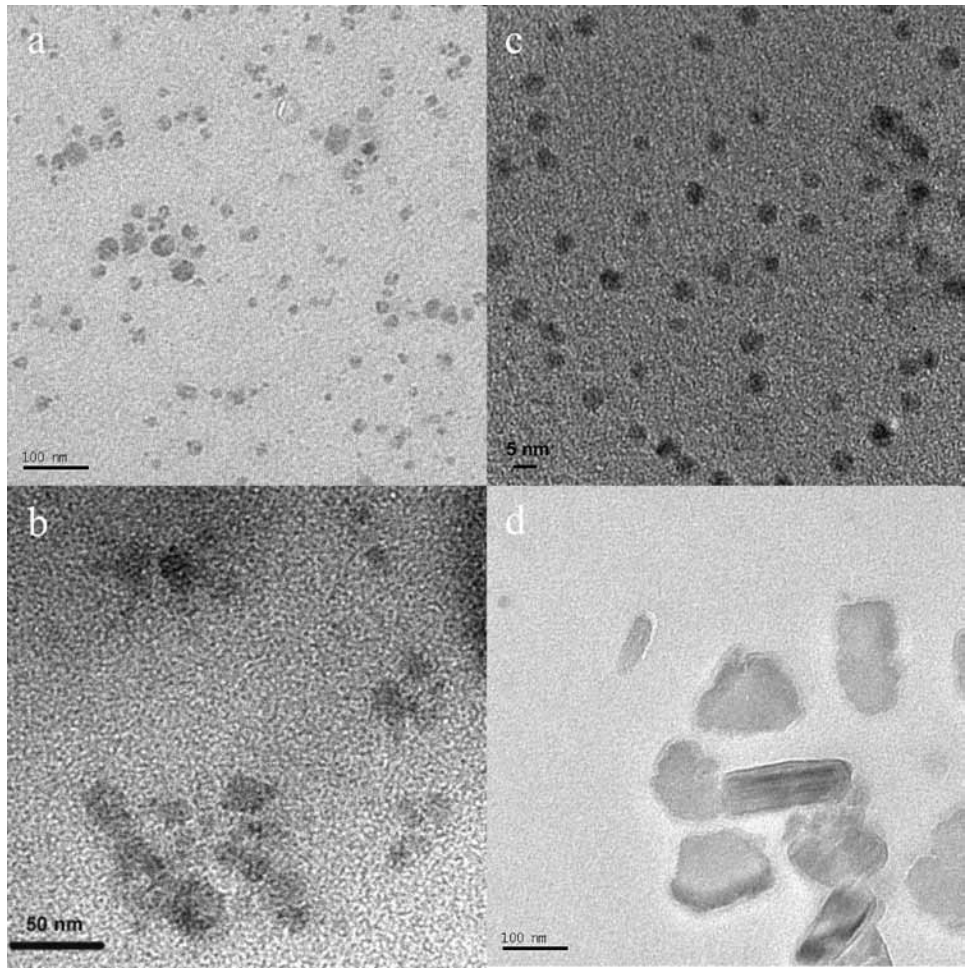

Figure 2. TEM Images of 0.22 μm filtered suspension of C_{60}[Tol] 15:85 Triton X-100:H_2O solution, showing (a) an average particle size of 18 nm, (b) a sampling of particles in the range of 10−40 nm in diameter, some of which show faceted edges, (c) some particles down to about 5 nm in size (which do not clearly show facets or evidence of crystallinity), and (d) large particles on the order of 100 nm without filtering, which clearly show facets, indicating crystalline structure.

computer-controlled optical delay and then focused into a sapphire plate to generate a white light continuum. The white light was then overlapped with the pump beam in a 2 mm quartz cuvette and then coupled into a CCD detector. Data acquisition was controlled by software. The chirp effects on the spectra were within experimental error; therefore, no chirp corrections were made.

Laser Flash Photolysis. Nanosecond transient absorption measurements were carried out by using the third harmonic (355 nm) of a Q-switched Nd:YAG laser (pulse width ca. 5 ns). Pulse fluences of up to 8 mJ cm^{-2} at the excitation wavelength were typically used. A detailed description of the laser flash photolysis apparatus has been published earlier.[77]

Z-Scan. Nanosecond open-aperture z-scan experiments[78] were performed by using the second harmonic (532 nm) of a Q-switched Nd:YAG laser. The laser was operated with a single longitudinal mode and spatially in a TEM_{00} mode, with an output beam that was Gaussian in both space and time (7.1 ns fwhm). The diffraction-limited beam was focused to a spot of 23.6 μm ($HWe^{-2}M$), for which the Rayleigh range, Z_R, is 3.3 mm. All samples were tested in spectroscopic quality quartz cuvettes with 1 mm optical path lengths, which are considered thin compared to Z_R.

Results and Discussion

Particle Characterization by TEM. Figure 2 shows TEM images at different magnifications of the C_{60}[Tol] 15:85 Triton X-100:H_2O suspension which had been filtered through a 0.22 μm syringe filter. The particles are polydisperse, with sizes falling mostly in the range of 10−50 nm. In general, the particle shapes trend from rather spherical to more faceted as the particle size increases. Particle sizing from 100 particles in Figure 2a showed an average particle size of 18 ± 7 nm. Because the molecular density of C_{60} is $1.44 \times 10^{21}/cm^3$,[74] an 18 nm diameter spherical cluster will contain approximately 4392 C_{60} molecules if the sphere exhibits crystalline packing (face centered cubic). Figure 2b shows particles ranging in size from approximately 10 to 40 nm. Figure 2c shows several C_{60} particles with sizes near 5 nm. Although lattice fringes were observed for particles larger than 20 nm, evidence of crystallinity was not obtained from small particles such as these. However, further data would be required to confirm any size dependence to the crystalline nature of C_{60} particles. Future efforts may employ X-ray diffraction of the sub 10 nm component of the toluene/triton/water assembled C_{60}. Figure 2d shows colloidal particles of approximately 100−150 nm diameter in the unfiltered C_{60} colloid suspension. These particles clearly exhibit facets and fringe patterns, indicating crystalline packing.

Figure 3 shows TEM images of a C_{60} colloidal particle from this suspension at high magnification, revealing faceted edges and parallel lines. As shown in the inset to Figure 3b, the diffraction pattern in the digital Fast Fourier Transform image is consistent with either face centered cubic or a hexagonal

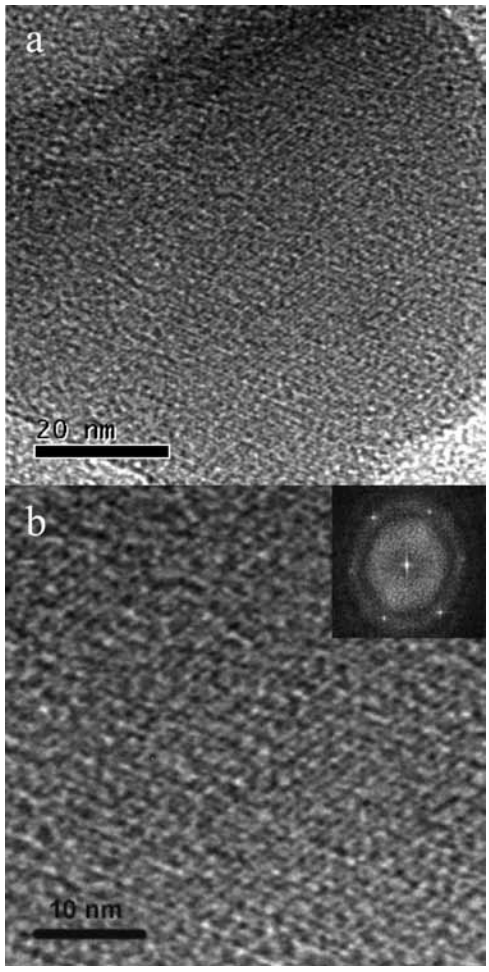

Figure 3. Higher-resolution TEM image of C_{60}[Tol] 15:85 Triton X-100:H_2O, showing (a) faceted perimeter and (b) lattice fringes. Inset is a Fourier-transform electron-diffraction pattern showing hexagonal crystal symmetry (possibly face centered cubic).

crystalline symmetry but was not sufficient to distinguish between these possible structures.

Particle-Size Distribution by DLS. Ultrapure deionized water (pH 7.5, 18 MΩ cm) was used to dilute the samples for DLS measurements. Table 1 shows particle-size data for both the unfiltered C_{60}[Tol] 15:85 Triton X-100:H_2O colloidal suspension and the same suspension after filtration through a 0.2 μm cellulose acetate filter and vacuum evacuation to remove bubbles that were caused by filtration. Data are presented in z-average, intensity, volume, and number bases. Although the visual appearance of the suspension changes from a cloudy brown to a clear brown upon filtration, the particle-size measurement by DLS are in close agreement before and after filtration (e.g., 106 versus 105 nm z-average before and after filtration). This is not altogether surprising, because the largest particles observed in the unfiltered colloidal suspension are on the order of 200 nm in diameter. Likewise, the small decrease in diameter from intensity to number basis argues against the presence of large outlier particles. Taken together with the TEM data, the sample may be said to consist of a fairly broad distribution of colloidal particles predominantly in the range of 10−100 nm in diameter. Although the average particle size of the acidified carbon black is somewhat smaller than the C_{60} colloids (e.g., 80 nm z-average), they are of similar scale.

Ground-State Absorbance. Shown in Figure 4 are the quantified ground-state absorbance spectra of the C_{60}[Tol] 15:85 Triton X-100:H_2O colloidal suspension compared to C_{60} in toluene. The band appearing at 336 nm in the C_{60} in toluene solution has shifted slightly to 342 nm in the colloidal suspension. This absorption band is known to be affected by its environment, and this red-shift suggests that the Triton X-100: water solution has stabilized the C_{60} slightly more than the toluene.[79] In addition, the overall absorption of this band has reduced in magnitude in the Triton X-100:Water suspension compared to the toluene solution. The band at 450 nm has been previously reported and attributed to aggregation of C_{60} within the Triton X-100 micelle.[65,66,79,80] The amount of aggregation is highly dependent on the preparation method of the colloidal suspension.[50,59,81,82] In the literature, Bensasson et al. found that preparation of the C_{60} micelles under nitrogen ($\varepsilon_{450nm} = 2100$ M^{-1} cm^{-1}) or oxygen ($\varepsilon_{450nm} = 12180$ M^{-1} cm^{-1}) led to different degrees of aggregation.[79] The C_{60}[Tol] 15:85 Triton X-100:H_2O sample was prepared under air-saturated conditions, and we observe a molar extinction coefficient of $\varepsilon_{450\ nm} = 4350$ M^{-1} cm^{-1}. When this experimental ε is plotted with the values from Bensasson versus percentage of oxygen (0, 21, 100), a linear fit is obtained. This indicates that preparation of these samples under varying oxygen concentrations allows tuning of the amount of colloidal C_{60} micelles present. Thus, the sample consists of a mixed colloidal suspension of both micelles with monomeric C_{60} and micelles containing colloidal particles of many C_{60} molecules.[79] The possibility that the mixture contains free C_{60} can be ruled out because of its very low solubility in water.[83−85] Also of note is the small bump observed at 615 nm in the colloidal suspension, which is consistent with the absorption peak observed at 599 nm for C_{60} in toluene (Inset of Figure 4). This red shift is also consistent with a greater stabilization of the energy by the colloidal suspension than the toluene solution. Overall, the ground-state absorption spectrum appears to contain a mixed absorption from the monomeric micelles and the colloidal micelles.

Time-Resolved Excited-State Properties. ***Ultrafast Transient Absorption.*** Femtosecond transient absorption measurements were conducted on the C_{60}[Tol] 15:85 Triton X-100:H_2O sample. A sample of C_{60} in air-saturated 15:85 Triton X-100: water was diluted to 988 μM for measurement, and the resulting data is shown in Figure 5. The times shown represent changes in the spectral data with decay. The lifetimes upon absorption of the 170 fs pulse were determined by using a multi exponential fit and are given in Table 2 for the air-saturated solution. For comparison, data for a sample of 938 μM C_{60} in air-saturated toluene is shown in Figure 6, and the lifetimes measured for C_{60} in toluene are given in Table 2. In C_{60} in toluene, the typical behavior reported in the literature was observed.[12] Upon absorption of the 390 nm pulse, a fast decay of 0.58 ps was observed that we attribute to intramolecular vibrational relaxation (IVR). This usually occurs within 1 ps and is due to relaxation from higher electronic and vibrational levels back down to the lowest vibrational level of the S_1 state. This was also observed in the C_{60}[Tol] 15:85 Triton X-100:H_2O sample. The second observed lifetime of 8.0 ps is most likely due to solvent reorganization around the C_{60} in toluene. The time scale is consistent with this. A similar process was observed in the C_{60} colloidal sample with a lifetime of 5.3 ps. The first two lifetimes for both samples are very close to each other, indicating that the aggregated colloidal structure has no effect on these processes. The third lifetime observed in C_{60} in toluene is due to formation of the triplet excited state via intersystem crossing. This is well known in the literature to be 1200 ps, and our measurement is within error of this value.[12] The data collected for the C_{60}[Tol] 15:85 Triton X-100:H_2O indicate a lifetime of

TABLE 1: Particle Size Data for C_{60} Colloids in Triton X-100:Water Solutions

	z-average (nm)		intensity (nm)		volume (nm)		number (nm)	
	APS[b]	PDI[c]	APS	PW[d]	APS	PW	APS	PW
C_{60}[Tol] 15:85 Triton X-100:H_2O unfiltered (refractive index = 2.2)	106	0.219	131	55.2	101	53.3	64.5	21.1
C_{60}[Tol] 15:85 Triton X-100:H_2O filtered (0.2 μm)[a] (refractive index = 2.2)	105	0.25	117	39.7	94.9	37.4	70.3	19.9
acidified carbon black in water unfiltered (refractive index = 1.85)	79.9	0.197	102	51.8	67.1	48.6	37.5	13.6

[a] Filtered through a 0.2 μm cellulose acetate filter. [b] Average particle size. [c] Polydispersity index. [d] Peak width.

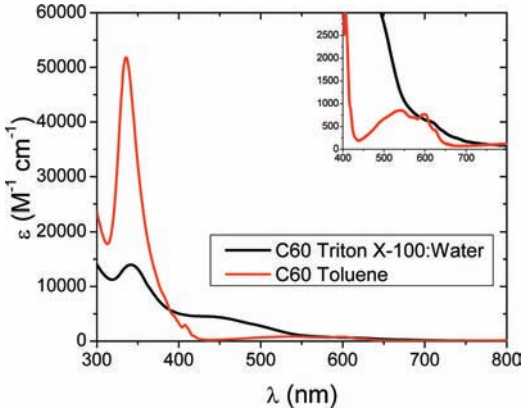

Figure 4. Quantified UV−vis absorbance spectra of C_{60} colloid suspension in 15:85 Triton X-100:water compared to C_{60} in toluene. Inset shows rescaled region from 400−800 nm to accentuate absorption features in this region.

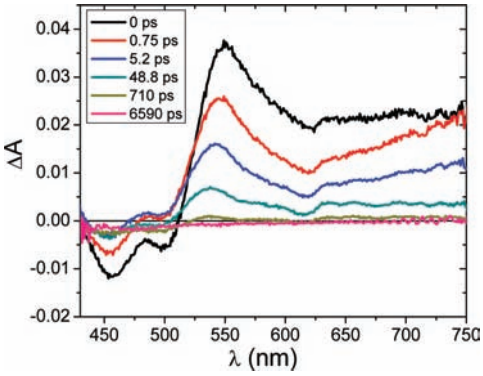

Figure 5. Transient absorption of 988 μM air-saturated C_{60} colloid suspension in 15:85 Triton X-100:water upon 390 nm absorption of a 170 fs pulse. Times shown are 0, 0.75, 5.2, 48.8, 710, and 6590 ps immediately following the laser pulse.

TABLE 2: Kinetic Lifetimes of C_{60} Colloids in 15:85 Triton X-100:Water and C_{60} in Toluene

	C_{60}[Tol] 15:85 Triton X-100: H_2O	C_{60} in toluene
τ_1	0.53 ± 0.28 ps[a]	0.58 ± 0.52 ps[a]
τ_2	5.3 ± 1.8 ps[a]	8.0 ± 4.7 ps[a]
τ_3	42.6 ± 13.2 ps[a]	960 ± 380 ps[a]
τ_4	Long tail, 1.1 μs[b] 86 μs[c]	Long tail, 333 ns[b] 3.7 μs[c]

[a] 390 nm 170 fs excitation (sample air saturated). [b] 355 nm 5 ns excitation (sample air saturated). [c] 355 nm 5 ns excitation (sample deoxygenated via freeze pump thaw).

42.6 ps, which is significantly shorter than that of the C_{60}/toluene sample. On the basis of studies done on solid films of C_{60}, we believe that this shortened lifetime is due to quenching of the singlet excited state through either a self-quenching process or singlet−singlet annihilation.[17,86] Within a micelle, there could be two or more C_{60} molecules present, eliminating any slow diffusional processes and leading to very efficient quenching

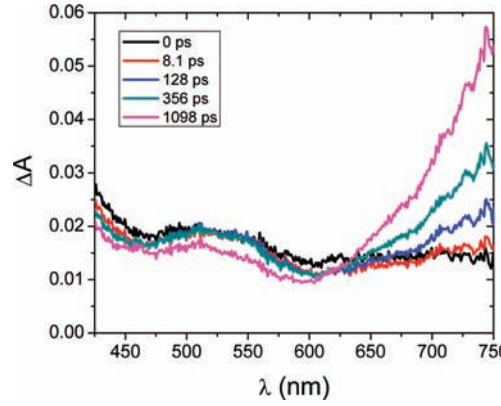

Figure 6. Transient absorption of 938 μM C_{60} in air-saturated toluene following 390 nm absorption. Shown are times immediately following the 170 fs laser pulse of 0, 8.1, 128, 356, and 1098 ps.

of the C_{60} singlet excited state. A long tail absorption was also measured for the C_{60}[Tol] 15:85 Triton X-100:H_2O sample. This long tail of transient absorption might be due to formation of the triplet excited state or formation of reduced C_{60} ($C_{60}^{\bullet-}$) in a self-quenching reaction.[87] The spectrum at this probe delay is not consistent with triplet C_{60}, but the weak absorption signal was near the limit of detection. Because our apparatus was unable to measure beyond 800 nm, we were unable to confirm a $C_{60}^{\bullet-}$ absorption feature at 1070 nm. Therefore, we were not able to properly assign this species. For C_{60} in toluene, a long-lived transient with a peak at 740 nm was observed, which is consistent with the triplet excited-state absorption.[12] In the literature, there have been several ultrafast transient absorption studies done on thin films of C_{60}[27,88] that reveal spectral properties similar to those measured in Figure 5, indicating that the colloidal sample is acting much like a solid film. In both cases, the authors describe the transient absorption as coming from formation of a singlet exciton. In addition, a study on a C_{60} film excited at 633 nm resulted in three lifetimes of τ_1 = 0.26 ps, τ_2 = 4.6 ps, and τ_3 = 64 ps,[25] which are similar to what we found for the colloidal sample.

Overall, the femtosecond data reveal that a quenching process is occurring in the C_{60} colloidal sample at a fast rate, nearly eliminating intersystem crossing to the triplet excited state. By using the lifetimes collected, the following calculation was performed to estimate the fraction of singlet excited state quenched. By assuming a pseudo first-order rate and knowing that the k_{obs} value of the colloidal sample is 2.3×10^{10} s^{-1} (1/42.6 ps), k_d is 1.0×10^9 s^{-1} (1/960 ps) from the C_{60} in toluene, and the concentration of quencher is 988 μM (i.e., the concentration of C_{60} in the diluted suspension), we use eq 3 to determine the rate constant for quenching k_q (M^{-1} s^{-1}) to be 2.2×10^{13} M^{-1} s^{-1}.

$$k_{obs} = k_d + k_q[Q] \quad (3)$$

The rate constant determined is much faster than a typical diffusion controlled rate constant of 1×10^9 M^{-1} s^{-1} because

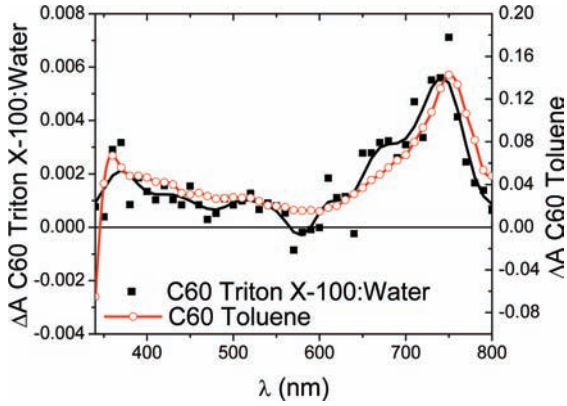

Figure 7. Shown are overlaid transient absorption spectra of 44.1 μM C_{60} colloid in 15:85 Triton X-100:water and 17.0 μM C_{60} in toluene immediately following 355 nm nanosecond excitation in air-saturated solution. Samples have matched OD at 355 nm of 0.435. Axes show the actual ΔA values measured.

of the packing of the C_{60} molecules within the micelle, eliminating any diffusion. The estimated fraction of singlet excited states quenched by using this calculation is 95.6% in the colloidal sample.

Laser Flash Photolysis. To further confirm that only small quantities of the triplet excited state are produced upon irradiation in the C_{60}[Tol] 15:85 Triton X-100:H_2O sample, nanosecond laser flash photolysis was also performed. The sample was excited at 355 nm with a 5 ns pulse. For comparison purposes, laser flash photolysis of C_{60} in toluene was also conducted. Both samples had a matched OD at 355 nm, so that the overall absorption could be compared between the two samples. For both samples, data was taken under both air-saturated and deoxygenated conditions. Shown in Figure 7 is data collected immediately after the laser pulse for 17.0 μM C_{60} in air-saturated toluene and 44.1 μM C_{60} in air-saturated 15:85 Triton X-100:water. The lifetimes are given in Table 2. The shapes of the spectra are nearly identical with only a small shift in the maximum peak. The magnitude of the change in absorbance, ΔA, however, is markedly different. With a matched OD at the exciting wavelength, the same number of singlet excited states are produced in each sample. However, in the C_{60}[Tol] 15:85 Triton X-100:H_2O, the ΔA at the peak of the spectrum is 0.006, whereas for C_{60} in toluene, the ΔA is 0.143 at the peak. This 96% lower magnitude in the change of absorbance in the C_{60}[Tol] 15:85 Triton X-100:H_2O as compared to the solution of C_{60} in toluene is consistent with our estimate of the fraction of excited singlet states quenched (95.6%). Therefore, there is still a small percentage (~4%) of C_{60} singlet excited states undergoing intersystem crossing to the triplet excited state.

The laser flash photolysis data for C_{60} in deoxygenated 15:85 Triton X-100:water did not result in a measurable spectrum; the only discernible signal appeared at 740 nm. From the weak 740 nm peak, we were able to extract a lifetime of 86 μs for the deoxygenated sample. We observe a measurable triplet excited-state spectrum for C_{60} colloids under air-saturated conditions, but under deoxygenated conditions, the transient formed is of much lower magnitude. The sample was deoxygenated via three freeze−pump−thaw cycles. The ground-state absorption spectrum was carefully monitored before and after deoxygenation, and there were no significant changes—particularly in the broad region near 450 nm which is attributed to the presence of the colloidal particles—indicating that the sample had not changed. We hypothesize that a possible explanation for this observation may be that there is a slight competition by trapped oxygen to quench the singlet excited states. In other words, the rate of oxygen quenching of singlet C_{60} is much slower than the rapid self-quenching resulting from the close proximity of the C_{60} molecules, but it remains a competitive pathway under air-saturated conditions. Upon removal of this competitive reaction, the faster self-quenching pathway depletes the singlet excited states much more efficiently (to >96%), reducing the number of singlet excited states that intersystem cross to the triplet excited state.

Z-Scan. Open aperture z-scans were performed on three different material samples to investigate the presence of possible nonlinear optical behavior of the C_{60} colloids in the nanosecond regime. Two of those materials were performed as baselines to which to compare the colloid sample.

As a first baseline, z-scans of C_{60} in toluene were performed. A solution of 0.27 g/L of C_{60} in toluene was prepared and placed in a 1 mm path length quartz cuvette. An absorption coefficient of 0.696 cm^{-1} was measured at 532 nm in a spectrophotometer. The sample was immersed in a sonicator bath for 0.5 h and remeasured. The absorption coefficient remained constant. The sample was placed at the focus of the z-scan experiment, and we observed the transmission of the sample as a function of pulse number at both 10 Hz and 1 Hz to make sure that there was no multiple shot bleaching of the material. Because there did not appear to be such an effect occurring with the C_{60} sample, multiple z-scans were taken at 10 Hz, between energies of 0.26 and 2.41 μJ (Figure 8a). Each point of the z-scan represents an average of 25 shots at each z-position. In addition, each z-scan was background corrected. Simplified three-level analysis was performed on the data as in Wood et al.[89] for each input energy, and the average triplet cross section was determined to be 7.5×10^{18} cm^2, which is very close to the value of 8.1×10^{18} cm^2 measured previously by Ebbesen et al.[12] and slightly lower, as would be expected because of the assumptions of our relatively simple analysis. The z-scans on C_{60} in toluene are shown in Figure 8a.

Z-scans of acidified carbon in water were performed as a second baseline. The particle size distribution of the carbon black aggregates in this suspension were on average slightly smaller on a number-weighted basis than the colloidal C_{60} particles but were on the same order. (See Table 1.) The internal transmission of this sample was 9% at 532 nm. The nonlinear behavior of carbon black suspensions (CBS) is well documented and, at nanoseconds, is a nonlinear scattering effect caused by the linear absorption of incident light, followed by rapid heating and ionization of the carbon particle within the time scale of the pulse width.[90,91] After plasma formation, the remaining light in the pulse is scattered ala Mie scattering. Nonlinear scattering is the dominant mechanism exhibited by CBS, as well as for other carbon particle morphologies such as single and multiwall carbon nanotubes.[92] Studies have shown that open-aperture z-scans of carbon suspensions roughly resemble that of nonlinear absorbers,[93,94] although we know of no simple analysis to derive any photophysical properties from such a z-scan. When a z-scan is performed on CBS, there is a characteristic dip of the transmitted irradiance, but the dip is much narrower than that of a reverse saturable absorber (RSA) or two-photon absorber (TPA) material with the same change in transmitted irradiance and is caused by the scattering mechanism changing from Rayleigh to Mie as the fluence in the sample is increased. The input energy was varied between 5.5 and 11.8 μJ. Because bleaching of the sample began after each shot, no averaging was performed, and a delay of 200−500 s was introduced

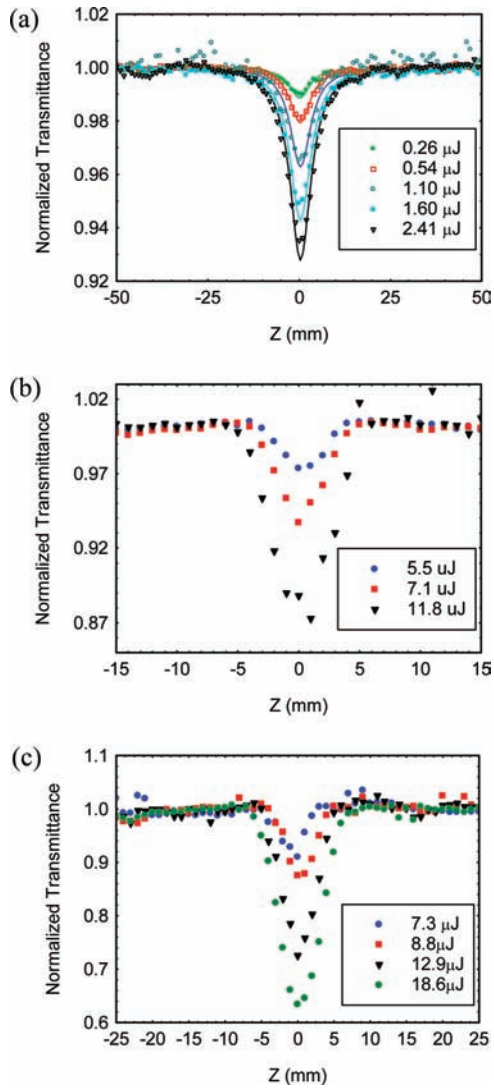

Figure 8. Z-scan of C_{60}[Tol] 15:85 Triton X-100:H_2O and benchmark materials at varying input energies. (a) C_{60} in toluene: simplified three-level analysis yields an average triplet cross section of 7.5×10^{18} cm^2. (b) Acidified carbon black in water: the data do not fit reverse saturable absorption theory. Carbon black suspensions are dominated by nonlinear scattering. (c) C_{60}[Tol] 15:85 Triton X-100:H_2O: the data do not fit reverse saturable absorption theory. The nonlinear response exhibited by this material is dominated by scattering.

between each z-position. The results of the z-scans on acidified carbon in water are shown in Figure 8b. The dip of the open aperture z-scan of acidified carbon is much narrower than that of the reverse saturable absorption exhibited by the C_{60} sample, did not fit three-level analysis models of RSA behavior, and is consistent with the nonlinear scattering mechanism of CBS.

Z-scans of the C_{60}[Tol] 15:85 Triton X-100:H_2O sample were performed. The internal cell transmittance in a 1 mm quartz cuvette was 24.5% at 532 nm. As with the acidified carbon, bleaching was clearly evident after each pulse, and recovery time was greater than 15 min. In these z-scans, the energy was varied between 7.3 and 18.6 μJ. Each point in Figure 8c represents one shot. The cell was translated at least 500 μm vertically or horizontally between each shot so as to provide an unbleached volume to the laser pulse. As can be seen from the data, the narrow dip of the z-scan for all energy levels tested indicates that nonlinear scattering is the dominant mechanism for this C_{60} colloid sample. The z-scan data did not fit three-level RSA analysis but was consistent with z-scans of CBS. Unfortunately, the poor signal-to-noise ratio of the unaveraged data limited the extent to which we could reduce the input energy. The weak triplet−triplet absorption observed for this sample in the nanosecond flash photolysis experiment was below the noise floor of the z-scan experiment.

Conclusions

A sample of C_{60} colloids suspended in a micellar solution of 15:85 Triton X-100:water was produced by a modification of the method published by Deguchi,[44,63] resulting in a concentrated, somewhat polydisperse population of colloidal C_{60} particles, with particle diameters predominantly in the range of 10−100 nm, according to TEM and DLS measurements. The ground-state absorption spectrum of this sample showed a broad feature centered at 450 nm, indicative of the presence of colloidal C_{60} particles.

Femtosecond transient absorption spectroscopy experiments with 390 nm 170 fs excitation elucidated decay lifetimes of 0.53 ps due to IVR, 5.3 ps due to solvent reorganization around the C_{60}, 42.6 ps due to quenching of the singlet excited state by either a self-quenching process or singlet−singlet annihilation, and a long-lived absorption which may be due to either a triplet excited state or formation of reduced C_{60} ($C_{60}^{\bullet -}$) in a self-quenching reaction. This contrasts with a 0.96 ns intersystem crossing (ISC) to the triplet excited state and a long-lived triplet state in a solution of C_{60} in toluene. Similarities of the transient spectrum and decay rates to studies of thin films of C_{60}[25,27,86] indicate that at this level of aggregation, the colloidal C_{60} particles behave optically much like bulk C_{60}. It is estimated that 95.6% of the singlet excited states are quenched.

Nanosecond laser flash photolysis experiments show that the C_{60}[Tol] 15:85 Triton X-100:H_2O sample produces a transient change-in-absorbance spectrum that is nearly identical to the triplet excited-state absorption of a solution of C_{60} in toluene, but approximately 96% reduced in magnitude. This is consistent with our estimate of the proportion of singlet states quenched and indicates that there is indeed some intersystem crossing to the triplet excited state occurring. Of interest is that this triplet-state formation was observed to a greater extent in the air-saturated sample than in a deoxygenated sample. We hypothesize that this is due to a slight competition by trapped oxygen to quench the singlet excited states and that when the oxygen is removed, the more rapid self-quenching pathway in the colloidal micelles more efficiently depletes the singlet excited states, reducing intersystem crossing.

Z-scan analysis served to confirm that the C_{60}[Tol] 15:85 Triton X-100:H_2O sample was dominated in its optical response by nonlinear scattering. Although the flash photolysis results indicate that some reverse saturable absorption behavior is indeed present in this material, its magnitude was below the detection threshold of the z-scan experiment.

Acknowledgment. The authors thank Anthony Sutorik of Army Research Laboratory for helpful discussions.

Supporting Information Available: Additional TEM data showing the unfiltered colloidal C_{60} suspension. DLS data for both filtered (0.2 μm) and unfiltered colloidal C_{60} suspensions, plotted on intensity, volume, and number distribution bases. This material is available free of charge via the Internet at http://pubs.acs.org.

References and Notes

(1) Kroto, H. W.; Heath, J. R.; Obrien, S. C.; Curl, R. F.; Smalley, R. E. *Nature* **1985**, *318*, 162.

(2) Zhang, P.; Lu, J.; Xue, Q.; Liu, W. *Langmuir* **2001**, *17*, 2143.
(3) Kelty, S. P.; Chen, C. C.; Lieber, C. M. *Nature* **1991**, *352*, 223.
(4) Kaiser, M.; Reichenbach, J.; Byrne, H. J.; Anders, J.; Maser, W.; Roth, S.; Zahab, A.; Bernier, P. *Synth. Met.* **1992**, *51*, 251.
(5) Lee, C. H.; Yu, G.; Moses, D.; Srdanov, V. I.; Wei, X.; Vardeny, Z. V. *Phys. Rev. B* **1993**, *48*, 8506.
(6) Minami, N. *Mol. Cryst. Liq. Cryst.* **1992**, *216*, 499.
(7) Yonehara, H.; Pac, C. *Appl. Phys. Lett.* **1992**, *61*, 575.
(8) Kamat, P. V.; Haria, M.; Hotchandani, S. *J. Phys. Chem. B* **2004**, *108*, 5166.
(9) Jensen, A. W.; Wilson, S. R.; Schuster, D. I. *Bioorg. Med. Chem.* **1996**, *4*, 767.
(10) Bosi, S.; Da Ros, T.; Spalluto, G.; Prato, M. *Eur. J. Med. Chem.* **2003**, *38*, 913.
(11) Nakamura, E.; Isobe, H. *Acc. Chem. Res.* **2003**, *36*, 807.
(12) Ebbesen, T. W.; Tanigaki, K.; Kuroshima, S. *Chem. Phys. Lett.* **1991**, *181*, 501.
(13) Sension, R. J.; Phillips, C. M.; Szarka, A. Z.; Romanow, W. J.; McGhie, A. R.; McCauley, J. P.; Smith, A. B.; Hochstrasser, R. M. *J. Phys. Chem.* **1991**, *95*, 6075.
(14) Blau, W. J.; Byrne, H. J.; Cardin, D. J.; Dennis, T. J.; Hare, J. P.; Kroto, H. W.; Taylor, R.; Walton, D. R. M. *Phys. Rev. Lett.* **1991**, *67*, 1423.
(15) Creegan, K. M.; Robbins, J. L.; Robbins, W. K.; Millar, J. M.; Sherwood, R. D.; Tindall, P. J.; Cox, D. M.; Smith, A. B.; McCauley, J. P.; Jones, D. R.; Gallagher, R. T. *J. Am. Chem. Soc.* **1992**, *114*, 1103.
(16) Bensasson, R. V.; Hill, T.; Lambert, C.; Land, E. J.; Leach, S.; Truscott, T. G. *Chem. Phys. Lett.* **1993**, *201*, 326.
(17) Fraelich, M. R.; Weisman, R. B. *J. Phys. Chem.* **1993**, *97*, 11145.
(18) Fujitsuka, M.; Watanabe, A.; Ito, O.; Yamamoto, K.; Funasaka, H. *J. Phys. Chem. A* **1997**, *101*, 7960.
(19) Klimov, V.; Smilowitz, L.; Wang, H.; Grigorova, M.; Robinson, J. M.; Koskelo, A.; Mattes, B. R.; Wudl, F.; McBranch, D. W. *Res. Chem. Intermed.* **1997**, *23*, 587.
(20) Arbogast, J. W.; Darmanyan, A. P.; Foote, C. S.; Rubin, Y.; Diederich, F. N.; Alvarez, M. M.; Anz, S. J.; Whetten, R. L. *J. Phys. Chem.* **1991**, *95*, 11.
(21) Nakamura, A.; Ichida, M.; Yajima, T. *Prog. Cryst. Growth Charact.* **1996**, *33*, 169.
(22) Hebard, A. F.; Haddon, R. C.; Fleming, R. M.; Kortan, A. R. *Appl. Phys. Lett.* **1991**, *59*, 2109.
(23) Dravid, V. P.; Liu, S.; Kappes, M. M. *Chem. Phys. Lett.* **1991**, *185*, 75.
(24) David, W. I. F.; Ibberson, R. M.; Matthewman, J. C.; Prassides, K.; Dennis, T. J. S.; Hare, J. P.; Kroto, H. W.; Taylor, R.; Walton, D. R. M. *Nature* **1991**, *353*, 147.
(25) Rosker, M. J.; Marcy, H. O.; Chang, T. Y.; Khoury, J. T.; Hansen, K.; Whetten, R. L. *Chem. Phys. Lett.* **1992**, *196*, 427.
(26) Ichihashi, T.; Tanigaki, K.; Ebbesen, T. W.; Kuroshima, S.; Iijima, S. *Chem. Phys. Lett.* **1992**, *190*, 179.
(27) Ebbesen, T. W.; Mochizuki, Y.; Tanigaki, K.; Hiura, H. *Europhys. Lett.* **1994**, *25*, 503.
(28) Tanigaki, K.; Kuroshima, S.; Ebbesen, T. W. *Thin Solid Films* **1995**, *257*, 154.
(29) Ichida, M.; Sakai, M.; Yajima, T.; Nakamura, A. *Prog. Cryst. Growth Charact.* **1996**, *33*, 125.
(30) Cheville, R. A.; Halas, N. J. *Phys. Rev. B* **1992**, *45*, 4548.
(31) Halas, N. J.; Papanyan, V.; Averitt, R. D.; Pippenger, P.; Cheville, R. A. *Mol. Cryst. Liq. Cryst. Sci. Technol. Sect. A-Mol. Cryst. Liq. Cryst.* **1994**, *256*, 225.
(32) Dexheimer, S. L.; Vareka, W. A.; Mittleman, D.; Zettl, A.; Shank, C. V. *Chem. Phys. Lett.* **1995**, *235*, 552.
(33) Flom, S. R.; Bartoli, F. J.; Sarkas, H. W.; Merritt, C. D.; Kafafi, Z. H. *Phys. Rev. B* **1995**, *51*, 11376.
(34) Nakamura, A.; Ichida, M.; Yajima, T.; Shinohara, H.; Saitoh, Y. *J. Lumin.* **1995**, *66*−*7*, 383.
(35) Ying, Q.; Marecek, J.; Chu, B. *Chem. Phys. Lett.* **1994**, *219*, 214.
(36) Ying, Q. C.; Marecek, J.; Chu, B. *J. Chem. Phys.* **1994**, *101*, 2665.
(37) Nath, S.; Pal, H.; Palit, D. K.; Sapre, A. V.; Mittal, J. P. *J. Phys. Chem. B* **1998**, *102*, 10158.
(38) Nath, S.; Pal, H.; Sapre, A. V. *Chem. Phys. Lett.* **2002**, *360*, 422.
(39) Nath, S.; Pal, H.; Sapre, A. V. *Chem. Phys. Lett.* **2000**, *327*, 143.
(40) Bokare, A. D.; Patnaik, A. *J. Phys. Chem. B* **2005**, *109*, 87.
(41) Bokare, A. D.; Patnaik, A. *Carbon* **2003**, *41*, 2643.
(42) Bokare, A. D.; Patnaik, A. *J. Chem. Phys.* **2003**, *119*, 4529.
(43) Bokare, A. D.; Patnaik, A. *J. Phys. Chem. B* **2003**, *107*, 6079.
(44) Alargova, R. G.; Deguchi, S.; Tsujii, K. *J. Am. Chem. Soc.* **2001**, *123*, 10460.
(45) Ghosh, H. N.; Sapre, A. V.; Mittal, J. P. *J. Phys. Chem.* **1996**, *100*, 9439.
(46) Mrzel, A.; Mertelj, A.; Omerzu, A.; Copic, M.; Mihailovic, D. *J. Phys. Chem. B* **1999**, *103*, 11256.
(47) Rudalevige, T.; Francis, A. H.; Zand, R. *J. Phys. Chem. A* **1998**, *102*, 9797.
(48) Sun, Y. P.; Bunker, C. E. *Chem. Mater.* **1994**, *6*, 578.
(49) Sun, Y. P.; Bunker, C. E. *Nature* **1993**, *365*, 398.
(50) Fortner, J. D.; Lyon, D. Y.; Sayes, C. M.; Boyd, A. M.; Falkner, J. C.; Hotze, E. M.; Alemany, L. B.; Tao, Y. J.; Guo, W.; Ausman, K. D.; Colvin, V. L.; Hughes, J. B. *Environ. Sci. Technol.* **2005**, *39*, 4307.
(51) Sayes, C. M.; Fortner, J.; Lyon, D.; Ausman, K. D.; Guo, W. H.; Colvin, V. *Abstr. Pap. Am. Chem. Soc.* **2004**, *227*, U1564.
(52) Sayes, C. M.; Fortner, J. D.; Guo, W.; Lyon, D.; Boyd, A. M.; Ausman, K. D.; Tao, Y. J.; Sitharaman, B.; Wilson, L. J.; Hughes, J. B.; West, J. L.; Colvin, V. L. *Nano Lett.* **2004**, *4*, 1881.
(53) Sayes, C. M.; Gobin, A. M.; Ausman, K. D.; Mendez, J.; West, J. L.; Colvin, V. L. *Biomaterials* **2005**, *26*, 7587.
(54) Markovic, Z.; Todorovic-Markovic, B.; Kleut, D.; Nikolic, N.; Vranjes-Djuric, S.; Misirkic, M.; Vucicevic, L.; Janjetovic, K.; Isakovic, A.; Harhaji, L.; Babic-Stojic, B.; Dramicanin, M.; Trajkovic, V. *Biomaterials* **2007**, *28*, 5437.
(55) Lee, J.; Fortner, J. D.; Hughes, J. B.; Kim, J. H. *Environ. Sci. Technol.* **2007**, *41*, 2529.
(56) Andrievsky, G. V.; Klochkov, V. K.; Bordyuh, A. B.; Dovbeshko, G. I. *Chem. Phys. Lett.* **2002**, *364*, 8.
(57) Andrievsky, G. V.; Klochkov, V. K.; Karyakina, E. L.; McHedlov-Petrossyan, N. O. *Chem. Phys. Lett.* **1999**, *300*, 392.
(58) Andrievsky, G. V.; Kosevich, M. V.; Vovk, O. M.; Shelkovsky, V. S.; Vashchenko, L. A. *J. Chem. Soc., Chem. Commun.* **1995**, 1281.
(59) Brant, J.; Lecoanet, H.; Hotze, M.; Wiesner, M. *Environ. Sci. Technol.* **2005**, *39*, 6343.
(60) Dhawan, A.; Taurozzi, J. S.; Pandey, A. K.; Shan, W. Q.; Miller, S. M.; Hashsham, S. A.; Tarabara, V. V. *Environ. Sci. Technol.* **2006**, *40*, 7394.
(61) Scrivens, W. A.; Tour, J. M.; Creek, K. E.; Pirisi, L. *J. Am. Chem. Soc.* **1994**, *116*, 4517.
(62) Ghosh, S. K.; Alargova, R. G.; Deguchi, S.; Tsujii, K. *J. Phys. Chem. B* **2006**, *110*, 25901.
(63) Deguchi, S.; Alargova, R. G.; Tsujii, K. *Langmuir* **2001**, *17*, 6013.
(64) Duncan, L. K.; Jinschek, J. R.; Vikesland, P. J. *Environ. Sci. Technol.* **2008**, *42*, 173.
(65) Beeby, A.; Eastoe, J.; Heenan, R. K. *J. Chem. Soc., Chem. Commun.* **1994**, 173.
(66) Hungerbuhler, H.; Guldi, D. M.; Asmus, K. D. *J. Am. Chem. Soc.* **1993**, *115*, 3386.
(67) Eastoe, J.; Crooks, E. R.; Beeby, A.; Heenan, R. K. *Chem. Phys. Lett.* **1995**, *245*, 571.
(68) Guldi, D. M.; Huie, R. E.; Neta, P.; Hungerbühler, H.; Asmus, K. -D. *Chem. Phys. Lett.* **1994**, *223*, 511.
(69) Guldi, D. M.; Hungerbuhler, H.; Asmus, K. D. *J. Phys. Chem. A* **1997**, *101*, 1783.
(70) Fujitsuka, M.; Kasai, H.; Masuhara, A.; Okada, S.; Oikawa, H.; Nakanishi, H.; Watanabe, A.; Ito, O. *Chem. Lett.* **1997**, 1211.
(71) Crooks, E. R.; Eastoe, J.; Beeby, A. *J. Chem. Soc. Faraday Trans.* **1997**, *93*, 4131.
(72) Sension, R. J.; Szarka, A. Z.; Smith, G. R.; Hochstrasser, R. M. *Chem. Phys. Lett.* **1991**, *185*, 179.
(73) The Dow Chemical Company. http://dow-answer.custhelp.com/cgi-bin/dow_answer.cfg/php/enduser/std_adp.php?p_faqid=1668&p_created=1084563836&p_topview=1.
(74) SES Research. Properties of Carbon 60, http://www.sesres.com/PhysicalProperties.asp.
(75) Weiner, B. B.; Tscharnuter, W. W.; Bernt, W. *J. Dispersion Sci. Technol.* **2002**, *23*, 671.
(76) Medalia, A. I.; Richards, L. W. *J. Colloid Interface Sci.* **1972**, *40*, 233.
(77) Rogers, J. E.; Cooper, T. M.; Fleitz, P. A.; Glass, D. J.; McLean, D. G. *J. Phys. Chem. A* **2002**, *106*, 10108.
(78) Sheik-Bahae, M.; Said, A. A.; Wei, T. H.; Hagan, D. J.; Van Stryland, E. W. *IEEE J. Quantum Electron.* **1990**, *26*, 760.
(79) Bensasson, R. V.; Bienvenue, E.; Dellinger, M.; Leach, S.; Seta, P. *J. Phys. Chem.* **1994**, *98*, 3492.
(80) Diederich, F.; Effing, J.; Jonas, U.; Jullien, L.; Plesnivy, T.; Ringsdorf, H.; Thilgen, C.; Weinstein, D. *Angew. Chem., Int. Edit. Engl.* **1992**, *31*, 1599.
(81) Brant, J. A.; Labille, J.; Bottero, J. Y.; Wiesner, M. R. *Langmuir* **2006**, *22*, 3878.
(82) Brant, J. A.; Labille, J.; Bottero, L. Y.; Wiesner, M. R. *Abstr. Pap. Am. Chem. Soc.* **2005**, *230*, U1544.
(83) Heymann, D. *Fullerene Sci. Technol.* **1996**, *4*, 509.
(84) Heymann, D. *Carbon* **1996**, *34*, 627.
(85) Ruoff, R. S.; Tse, D. S.; Malhotra, R.; Lorents, D. C. *J. Phys. Chem.* **1993**, *97*, 3379.
(86) Boucher, D.; Kovalenko, S. A.; Masselin, P.; Matveets, Y. A.; Novikov, M. G.; Ragulsky, V. V.; Stepanov, A. G.; Chekalin, S. V. *Izv. Akad. Nauk, Ser. Fiz.* **1998**, *62*, 237.

(87) Beeby, A.; Eastoe, J.; Crooks, E. R. *Chem. Commun.* **1996**, 901.
(88) Boucher, D.; Chekalin, S. V.; Kovalenko, S. A.; Matveets Yu, A.; Masselin, P.; Novikov, M. G.; Ragulsky, V. V.; Stepanov, A. G. *SPIE-Int. Soc. Opt. Eng.* **1997**, *3239*, 302.
(89) Wood, G. L.; Miller, M. J.; Mott, A. G. *Opt. Lett.* **1995**, *20*, 973.
(90) Mansour, K.; Soileau, M. J.; Vanstryland, E. W. *J. Opt. Soc. Am. B: Opt. Phys.* **1992**, *9*, 1100.
(91) Durand, O.; Grolir-Mazza, V.; Frey, R. *J. Opt. Soc. Am. B: Opt. Phys.* **1999**, *16*, 1431.
(92) Sun, X.; Xiong, Y. N.; Chen, P.; Lin, J. Y.; Ji, W.; Lim, J. H.; Yang, S. S.; Hagan, D. J.; Van Stryland, E. W. *Appl. Opt.* **2000**, *39*, 1998.
(93) Vivien, L.; Anglaret, E.; Riehl, D.; Hache, F.; Bacou, F.; Andrieux, M.; Lafonta, F.; Journet, C.; Goze, C.; Brunet, M.; Bernier, P. *Opt. Commun.* **2000**, *174*, 271.
(94) McEwan, K. J.; Milsom, P. K.; James, D. B. Nonlinear optical effects in carbon suspension. *Nonlinear Optical Liquids for Power Limiting and Imaging*; San Diego, CA, 1998.

JP8102518